Organic Solar cells, Dopants and Architectural Design – a Review

Seamus A. Curran[1,2], A. Haldar[2], Nigel Alley[1], Shawn Liao[1], James Dewald[2]

[1]CNTG, Dept of Physics, Science and Research Bld. 1, University of Houston, Houston, TX 77204, USA

[2]Dept of Physics, Science and Research Bld. 1, University of Houston, Houston, TX 77204, USA

Abstract

Since the discovery of conducting polymers by Alan Heeger, intensive research has been carried out over the last 50 years in order to find organic based molecular systems which would be suitable for electronic, photonic and all optical applications. Organic molecules possess desirable optical properties, while their responsiveness is such that the absorption and emission of such molecules can be tailored to specific needs. Polymers in particular have found a niche in transparent photovoltaic cells have for a number of years gathered considerable attention as an alternative to Cadmium Telluride (CdTe) or Copper Indium Gallium Diselenide (CIGS) or silicon solar cells, which is due to their relative low cost and ease of fabrication. In addition, given the flexibility to tailor the optical absorption through the availability of many different quantum dots, organic molecules, the potential to be able to engineer enhanced solar absorbance across the suns emission spectrum is one that is, while challenging, could be accomplished through techniques of blending and composite formation.

Introduction

The principle of operation for an organic photovoltaic (OPV) device is based on the conversion of incident electromagnetic radiation to electrical charges which may then be extracted at the

electrodes. There are a number of processes which occur in order to achieve this and the OPV architecture is an ensemble of planar layers engineered to carry out these processes as efficiently as possible. Essentially the OPV device layered structure is tailored to accommodate the so-called active-layer which typically comprises of one or more semiconductor materials which are either made up of organic materials that are solution processed or small molecular systems, which may be physically deposited by vapor deposition.

To understand how organics become interesting is to understand how a conjugated system works. Carbon has the ability to form 1, 2 and 3 bonded states, known as sp, sp2 and sp3 states. This is where it gets interesting, and that's looking at these states.

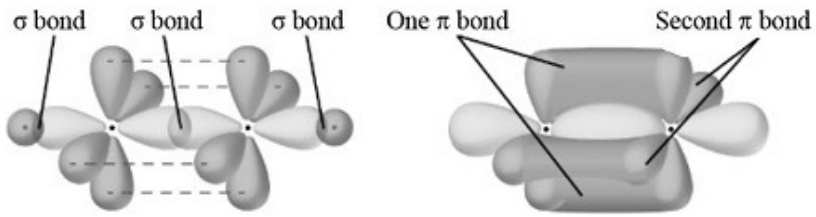

Figure 1 shows the different states of sigma and p orbitals.

In this case we can thank quantum where we see the atom is a very organized system with ordered hybridization. There is an idea that the universe is one filled with chaotic systems all scattered through the universe. According to the second law of thermodynamics the entropy of the university is always increasing. Another view to this is potential energy, imagine the universe is like a battery, as it cools down is like the energy being used up in kinetic energy. Eventually the universe will cool down to a balmy state of absolute zero also known as thermodynamic death. We know it is constantly changing where the universe is slowly cooling down and as such, electrons protons and neutrons could form, which then formed atoms we see in the periodic table. However, thermodynamics rescues us again when the 3rd law of

thermodynamics also states we cannot get to absolute zero. So, yet again the bewilderment of quantum comes to our rescue through the 3rd law.

The simplest π-conjugated polymer in existence is polyacetylene, which is composed entirely of carbon and hydrogen atoms. Conjugation denotes the sequence of alternating single and double bonds in the molecule. The structure of polyacetylene is shown in figure 1 and 2. (It is understood that each carbon atom also has a hydrogen atom bonded to it.)

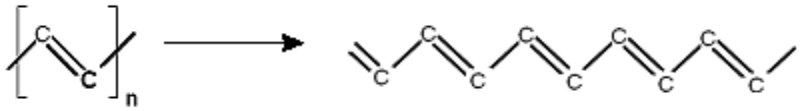

Figure 2: Structure of polyacetylene.

In a conjugated polymer, the atomic orbitals of the carbon atoms are hybridized, which means that the 2s orbital combines with the 2p orbitals to form new orbitals. In the case of polyacetylene and most other conjugated polymers, the carbon atoms undergo sp^2 hybridization. In this case the 2s orbital combines with the $2p_x$ and $2p_y$ (while the $2p_z$ orbital is unaffected) orbitals to form three sp^2 orbitals. These three sp^2 hybrid orbitals are energetically equivalent. They are also coplanar, directed 120° apart from each other (trigonal planar orbitals). These planar sp^2 orbitals are responsible for σ bonding to three neighbors. In the case of polyacetylene, two of these neighbors are carbon atoms, and one neighbor is a hydrogen atom. The fourth electron resides in the remaining (unaffected) p_z orbital, which lies perpendicular to the plane of the three sp^2 hybrid orbitals.[26] The spacing between carbon atoms is such that the p_z orbitals on adjacent carbon atoms overlap. Typically these p_z orbitals are referred to as π-orbitals, and the overlap of these neighboring p_z orbitals forms what is known as the π-bond. The π-bond creates a delocalized electron density above and below the plane of the carbon atoms, while the sp^2 orbitals

create highly localized electron densities in the plane of the carbon (and hydrogen) atoms. These delocalized π-orbitals are an important factor in the transport of charge.

The challenge with organic semiconducting materials is that they famously possess low mobility charge carriers when compared to their inorganic counterparts [8]. This imposes restrictions on device architecture which includes the thickness of the semiconductor layer, the blending process in formation of the heterojunction and the use of specific transparent electrode contacts. Poor exciton dissociation efficiency, related to small exciton diffusion lengths in conjugated polymers (5-20 nm) [9] leads to the requirement for an ultra-thin active layer film.

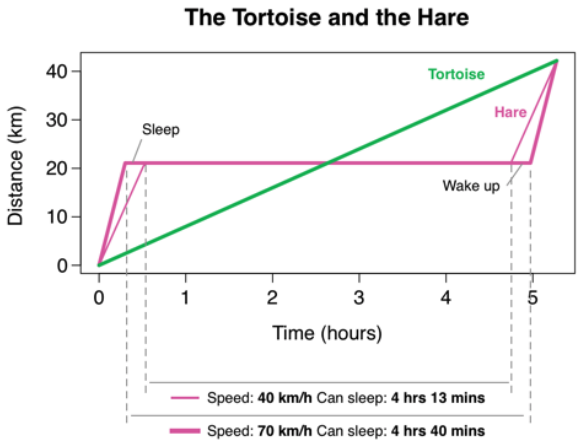

Figure 3: Exciton generation is almost instant while inorganics are slow in transition to an excited state. However, the inorganic exciton travels further than organics which generally fade quickly and travel short distances only.

Fullerenes have intrigued the world of organic research since their discovery in a wide variety of fields including physics, chemistry, materials science and biology. The potential of these materials, such as the use of C_{60} or C_{70} used as organic photovoltaics (blended or on their own) or carbon nanotube interconnects, have excited technologists worldwide. The chemistry of C_{60} and in particular the success of using C_{60} within blended composites for photovoltaics, shows a diversity in its electronic and chemical make-up, which enables scientists to use it for a multitude of applications [1-8].

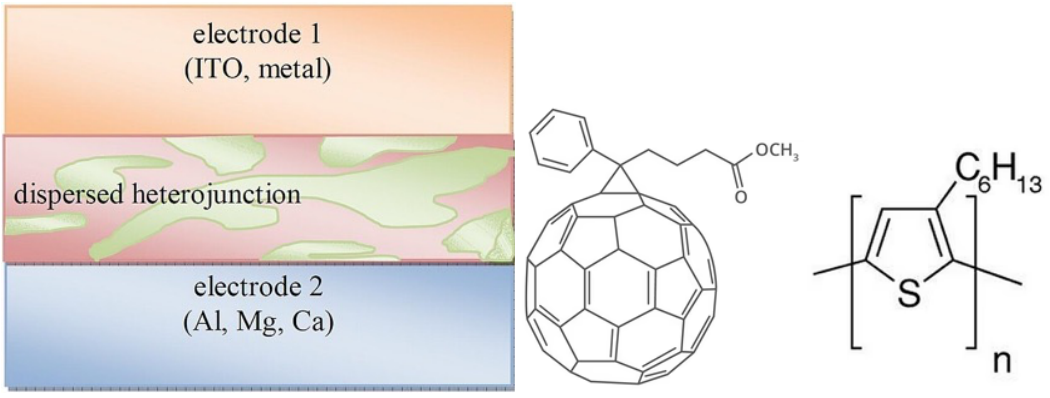

Figure 4: Doped fullerenes in the form of PCBM also act as n doped systems within p conjugated polymer systems. Shown here is a heterojunction, PCBM and P3HT adding to the complexity of OPV device fabrication.

In spite of the limitations of P3HT:PCBM based devices, power conversion efficiencies (PCEs) of around 5% have been achieved [9-11]. The success seen in PCE improvement for devices blended with Fullerenes is encouraging and investigating the role of Fullerenes in these systems to see how else we can modify them to improve PCE is of particular interest. Since the power conversions efficiency of blended polymer-fullerene nanocomposites achieved efficiencies of beyond 1% power conversion efficiency, organic photovoltaic research has focused on the need to go beyond the scope of interesting science and achieve practical uses of these novel nanomaterials. The power conversion efficiencies for the blended nanocomposites (5.2%) [12], while significantly higher than devices produced using traditional mixing (<1%), they are still far away from being economically practicable.

In order to develop much higher power conversion efficiency certain facets of the nanomaterial composition have to be taken account of. Current blended materials only use a small component of the sun's emission spectrum (mainly the visible), which means that substantial losses are already present within the device before any cell fabrication is carried out. Organic materials, while possessing certain semiconductor properties, also suffer from low

charge carrier capability. Consequently, when the exciton is generated (the electron-hole pair), the extent by which that exciton can travel has been calculated to be between 20 nm to 50 nm. In order to minimize the number of charge carriers lost to recombination, the organic semiconductor must remain relatively thin.

Absorption of a photon typically occurs practically instantaneously, on the order of a femtosecond. Typically, excitation is considered as occurring from the lowest vibrational level of the ground electronic state. Ultimately, the extra energy of the excited molecule is lost, with the molecule eventually returning to the lowest vibrational level of the ground electronic state. Typically, this involves some energy being converted to heat, and the rest of the energy being released in the form of an emitted photon, with energy less than the exciting photon. This photon emission is known as photoluminescence, of which there are two types; fluorescence and phosphorescence.

Experimental

Fabrication and electrical characterization of flat panel P3HT:PCBM photovoltaic cells fabrication procedure included a layer (~ 80 nm thick) of Poly(3,4-ethylenedioxythiophene):poly(styrenesulfonate) (PEDOT:PSS) (Baytron P) deposited onto cleaned ITO substrates (Delta Technologies, Rs = 10 Ω/sq.) by spin-coating. This layer was then dried at 80°C for 15 minutes. Next, a blend of regioregular P3HT (Aldrich, average molecular weight, Mw = 87 kg mol^{-1}) and PCBM (American Dye Source) was spin coated onto the PEDOT:PSS layer. Next, a lithium fluoride layer (~ 0.4 nm), and then an aluminum electrode layer (~ 80 nm) were thermally evaporated onto the P3HT:PCBM layer. The device was then removed from the evaporator and encapsulated using glass capsules with a silicon seal. Finally, after encapsulation, the device was annealed on a hot plate. Current density versus voltage (J-V)

measurements were acquired both in the dark and with illumination using a Keithley 236 voltage source/current measurement unit. For J-V measurements with illumination, the light source used was a calibrated AM1.5G solar simulator (Oriel), operating at 80 mW/cm^2.

Flat panel P3HT based photovoltaic devices were constructed as follows. First a commercially obtained indium tin oxide (ITO) sheet (40 Ω/sq. ITO on 125 μm thick polyester substrate, from Sheldahl, #155956) was affixed to a glass substrate (microscope slide). Then a solution of regioregular P3HT (poly(3-hexyl- thiophene-2,5-diyl), from American Dye Source Inc., #ADS306PT) (dissolved in toluene) was drop-cast onto the ITO layer and allowed to dry completely. This procedure was repeated multiple times until a relatively uniform (by visual inspection) thin film was formed. Then a vacuum evaporator was used to evaporate a layer of aluminum onto the P3HT layer. During the aluminum evaporation, a mask was used to block areas from aluminum evaporation. This was done to create multiple devices on a single flat panel structure. Finally, a small dab of silver paste was placed on top of each aluminum contact. This was done to prevent damage to the aluminum due to contact with the test probe. A simplified schematic diagram of one P3HT based photovoltaic device is shown in Figure 5, below.

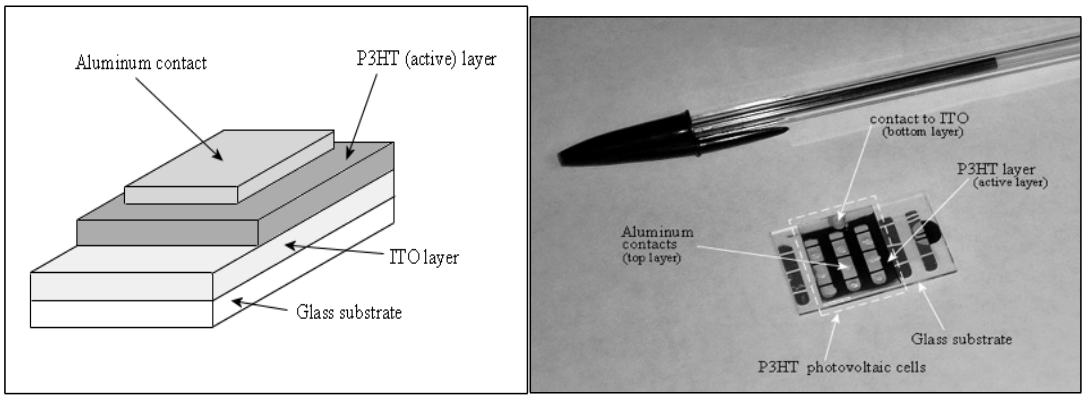

Figure 5: Schematic diagram of one P3HT based photovoltaic device on a flat panel structure. A photograph of a flat panel structure consisting of nine independent P3HT based photovoltaic cells is shown. A ball point pen is included in the photograph for scale.

These flat panel P3HT based photovoltaic devices were characterized via current density vs. voltage measurements both in the dark as well as under white-light illumination. A simplified schematic diagram of the experimental setup is shown in Figure 6. These flat panel P3HT based photovoltaic devices were characterized via current density vs. voltage measurements both in the dark as well as under white-light illumination. One electrical test lead was permanently attached (via silver paste) to the transparent indium tin oxide (ITO) layer of the device. Another test probe was used to make electrical contact with the aluminum contacts of the devices. A Keithley 6487 Picoammeter/Voltage source was used to provide a voltage sweep through the devices, while simultaneously measuring the current output. The devices were tested first with the room darkened. Subsequently, the devices were also tested under white light illumination white light illumination, a Leica white light source was used in line with the optical axis of the experimental setup. microParts UV/Vis microspectrometer via an optical fiber.

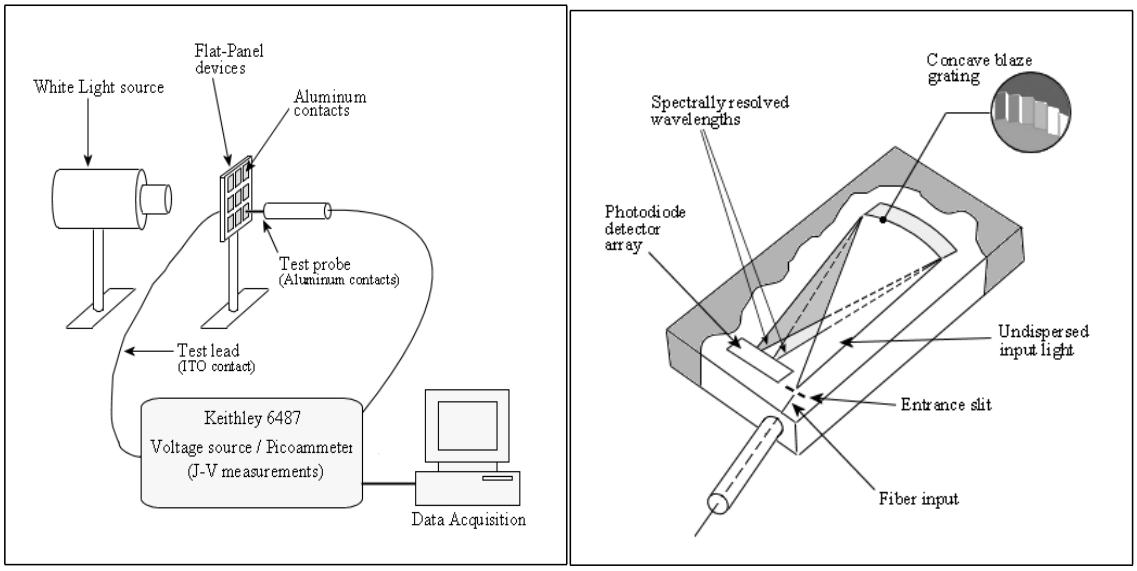

Figure 6: Simplified schematic diagram of the experimental setup used for characterization of the flat-panel P3HT photovoltaic devices.

One electrical test lead was permanently attached (via silver paste) to the transparent indium tin oxide (ITO) layer of the device. Another test probe was used to make electrical contact

with the aluminum contacts of the devices. A Keithley 6487 light collected via the optical fiber (300 μm core diameter) enters the cavity of the microspectrometer through a 50 μm x 300 μm entrance slit. The light is guided by total reflection inside the cavity of the spectrometer. This light is then incident upon a static concave blaze grating which disperses the incident light into a spectrum. This dispersed spectrum then strikes a Hamamatsu (S8378-256SPL) silicon-photodiode detector array. Unlike the Perkin-Elmer or Renishaw systems, this spectrometer has no moving parts, but rather measures spectra based upon which pixels on the detector array detect incident light.

Optical Absorption

To understand how the dynamic spin coating deposition method affects the thickness of the photoactive layers, the UV-Vis spectra of films fabricated under the same concentration both for P3HT and PCBM layers (PCBM 5 g/L, P3HT 10 g/L) were investigated. As shown in Figure 7, the absorption peak centered at 330 nm indicates the successful deposition of PCBM on the P3HT film using this method. According to the Beer-Lambert law which gives a relation between the absorbance and the film thickness, the deep peak density fall of chlorobenzene (b.p. 132 °C) treated film at 330 nm shows that the PCBM layer formed with this high boiling point solvent is notably thinner than the ones with lower boiling points (CH_2Cl_2 b.p. 40 °C; $CHCl_3$ b.p. 61 °C). This may be attributed to the higher surface tension of chlorobenzene, which hinders the PCBM solution from building up on top of the P3HT film during dynamic spin coating. During the solvent evaporation of a thin, spin-cast film, the P3HT 1-D polymer chains will self-organize in a lamellar structure, this is called intrachain or π-π^* stacking. The π-π^* stacking will introduce a difference in the UV-visible spectrum between the P3HT solution and dry film: a bathochromic shift in the absorption spectrum towards 515 nm (2.41 eV) can be observed. The three featured

vibronic absorption peak due to the P3HT π-π^* transitions are at 515 nm, 550 nm and 600 nm (2.25 and 2.07 eV). The peak intensity difference at 515 nm shows that the CH_2Cl_2 solution rarely affected the thickness of P3HT film (absorbance: A-P3HT/CH_2Cl_2 0.97, pristine P3HT normalized to 1), while $CHCl_3$ solution washed away about 30% of P3HT film (B-P3HT/$CHCl_3$ 0.74) and chlorobenzene solution around 50% (C-P3HT/chlorobenzene 0.49).

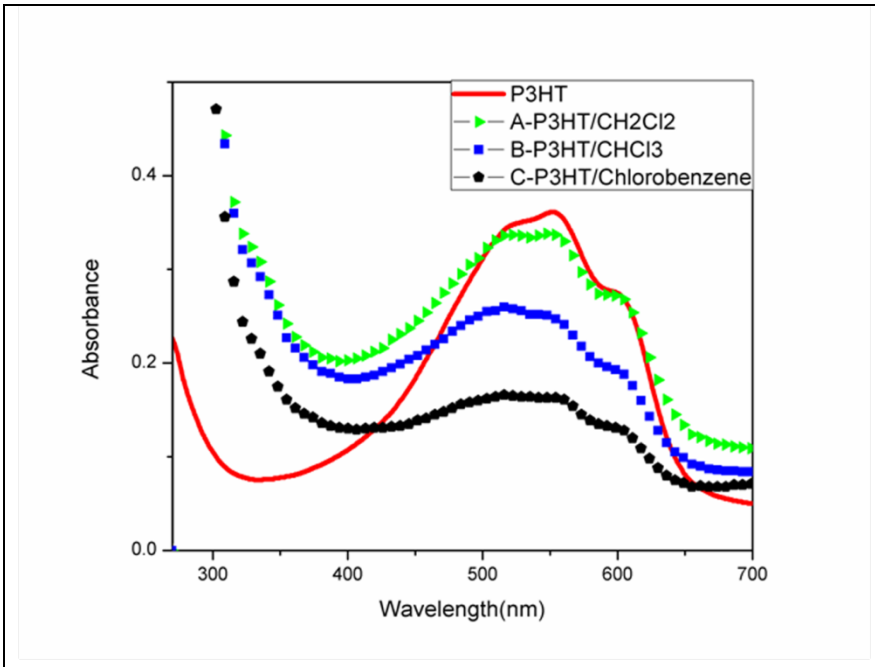

Figure 7: Absorption spectra of P3HT film (red line); P3HT film (10 g/L) spin coated with PCBM (5 g/L) in CH_2Cl_2 (green), $CHCl_3$ (blue) and chlorobenzene (black).

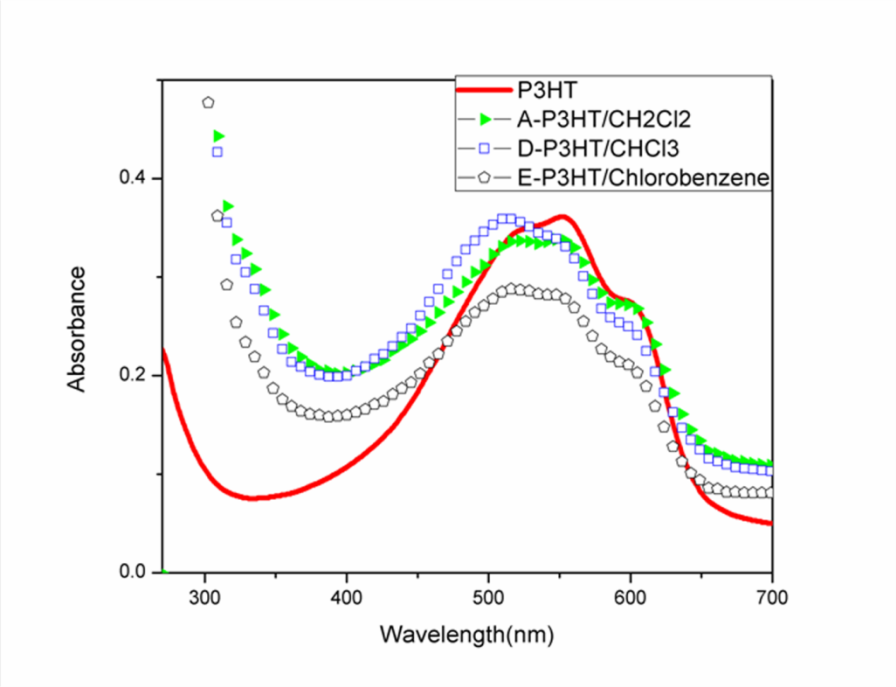

Figure 8. Absorption spectra of P3HT (10 g/L) film (red line); P3HT (10 g/L) spin coated with PCBM (5 g/L) in CH_2Cl_2 (green); P3HT (15g/L) with PCBM (5 g/L) in $CHCl_3$ (blue); P3HT (20 g/L) with PCBM (5 g/L) in chlorobenzene (black).

In order to correlate the cell performance with interface morphology generated by different solvents, we need to exclude the absorbance differences attributed to the P3HT layer. In this case another group with adjusted P3HT concentrations was fabricated and detailed parameters are listed in Table 1. Concentrations of P3HT are increased according to the UV-vis spectra. After the adjustment, a group of films with similar absorbance were obtained as shown in Figure 8.

	Sample	P3HT conc. (g/L)	Solvent for PCBM	Absorbance	Absorbance after normalizing
Group 1	A- CH_2Cl_2	10	CH_2Cl_2	0.34	0.97
	B- $CHCl_3$	10	$CHCl_3$	0.26	0.74
	C- chlorobenzene	10	Chlorobenzene	0.17	0.49
Group 2	A- CH_2Cl_2	10	CH_2Cl_2	0.34	0.97
	D- $CHCl_3$	15	$CHCl_3$	0.36	1.03
	E- chlorobenzene	20	Chlorobenzene	0.29	0.83
Pristine P3HT	10	Chlorobenzene	0.35	1	

Table 1. Absorbance at 515 nm of P3HT/PCBM films under different processing conditions.

The difference in the work functions of the two different conductors creates a built-in electric field. Under illumination, incoming photons can remove an electron from the polymer's valence band and promote it to the conduction band, creating an electron-hole pair, known as an exciton. The charge carriers can then drift in the built in electric field to their respective contacts. Electrons will move toward the lower work function metal, while the holes move to the higher work function metal. In this way, illumination in the device can create a current and it operates as a solar cell. However, most polymers, such as P3HT show primarily only hole transport and suffer from extremely low electron mobility. This makes effective dissociation of the photo generated excitons extremely difficult. Therefore, only those electron-hole pairs created very close to the low work function metal can be effectively separated to generate a photocurrent. Because of this, organic solar cells based solely on a polymer active layer typically exhibit very poor power conversion efficiencies. To overcome this problem, typically organic photovoltaics are constructed using a heterojunction in the active layer(s). This is done by using two different organic materials to comprise the active layer. The most common form is that of a polymer (typically P3HT) and fullerene molecules or functionalized fullerene molecules, such as PCBM.

In a heterojunction organic solar cell using a polymer and fullerenes, the polymer acts as the p-type semiconductor, while the fullerenes act as the n-type semiconductor. Another way to look at it is that the fullerene acts as an electron acceptor. In other words, when an incoming photon strikes the polymer, if it has sufficient energy, it can create an exciton (electron-hole pair). The electron can be liberated from the polymer and accepted by the fullerene molecule. Since the polymer possesses hole-transport properties, and the fullerenes exhibit electron transport properties, upon donating the electron to the fullerene, the photo generated excitons can be

effectively separated into separate charge carriers. Figure 9 illustrates the energy band structure for a polymer-PCBM heterojunction solar cell.

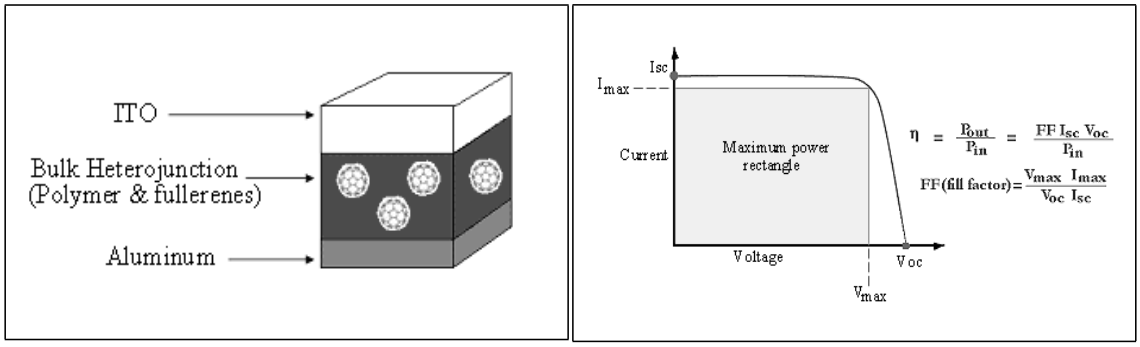

Figure 9: left) Diagram of a polymer-fullerene bulk heterojunction and right) Diagram of a polymer-fullerene bulk heterojunction.

However, if such a heterojunction is construct simply of a polymer layer in contact with a fullerene layer, efficient exciton separation will still be severely hampered, in a manner analogous to that of a pure polymer active layer. In other words, only those excitons created very close to the polymer-fullerene interface can be effectively separated into electrons and holes to generate a photocurrent. To overcome this, typically *bulk* heterojunctions are employed. This means that the fullerenes are dispersed throughout the polymer matrix, such that the entire active layer behaves as a heterojunction. A diagram illustrating a polymer-fullerene bulk heterojunction is shown in Figure 9. Obviously, the most important aspect of a solar cell is ability to convert light energy into electrical current. This is characterized by its power conversion efficiency, η, which is defined as the ratio of electrical output power to the optical power illuminating the device. The current-voltage characteristics (under illumination and forward bias), and relevant parameters used to characterize a solar cell device are illustrated in Figure 9.

The I-V curve shown in Figure 9 has been inverted; in other words, the absolute value of the current has been taken to create the curve shown. With illumination and under forward bias, the photocurrent would actually be negative, and the curve would actually occur in the fourth quadrant of an I-V graph. However, this does not change the theoretical treatment. The characterization of a solar cell's performance is as follows. The short-circuit current (Isc) is defined as the photocurrent generated with zero applied voltage, while the open-circuit voltage (Voc) is defined as the voltage that must be applied to cease any flow of current. Essentially, this is the built in potential created by the mismatch of the electrodes' work functions. As previously stated, the power conversion efficiency, η, is defined as the ratio of output power to input power where the output power, Pout, is defined as the maximum power point. This is the point on the I-V curve where the power, P = IV is at a maximum. The current and voltage values that correspond to Pmax are defined as Imax and Vmax, respectively. If lines are extended from this maximum power point to the axes of the I-V graph, what is known as the maximum power rectangle is defined, the area of which is the product of Imax and Vmax. Another parameter used to characterize solar cell device performance is known as the fill factor (FF).

The creation of an ordered nanophase structure that extends over several microns is a particularly important challenge for the nanosciences, in particular for organic-based materials. These are commonly referred to as "scaled structures" or "hierarchical structures" because structure can exist at many different length scales within them. It is believed that the ability to construct and arrange nanomaterials into three-dimensional arrays will provide the means to engineer novel new materials at the macroscale. It is well known that polymers are flexible and possess excellent optical absorption cross sections. These properties make them an attractive material for use in solar cells [13-19]. However, they suffer from a severe mismatch in length scale, strong fluorescence, and morphological control. The typical way of trying to overcome these problems is to create a "bulk-heterojunction" by dispersing nanostructured interfaces throughout the bulk

of the optically absorbing material. This helps to ensure that the excitons are efficiently separated into electrons and holes before recombination. The best-known nanomaterials to create these bulk heterojunctions are the fullerenes and their derivatives dispersed within a host polymer matrix. In the case of regioregular P3HT, holes are the high mobility carriers, so enhancing electron mobility (through the incorporation of fullerenes) also serves to provide charge balance to devices.

This approach has worked well in the past in terms of improving the efficiencies of polymer-based photovoltaics. However, in sub-percolating networks of fullerenes, hopping is the dominant process for electron mobility. This limit to the electron mobility detrimentally limits the overall maximum efficiencies that can be obtained from these devices. To tailor the carrier mobilities, it is necessary to better control the structure of the nanophase. In this work, the attempt was to create crystalline structures of PCBM that point toward the cathode (but not touching it) from the anode. This should provide an increase in the electron mobility that would more closely match the hole mobility of the P3HT. The enhancement of the photovoltaic device efficiency is caused in part by overall increase in the absorption. Current transport at a metal semiconductor junction is primarily due to majority carriers. The Schottky barrier diode equation describes the charge transport of an ideal metal semiconductor rectifying contact, and is expressed as:

$$J = Jo \, Exp \, (PV/nkT)$$

where J is the total current density, Jo is the reverse saturation current density, q is the electron charge, V is the applied voltage, n is the diode ideality factor, k is the Boltzmann constant, and T is the absolute temperature. Thermionic emission/diffusion (diffusion theory of current) theory gives an explicit relationship between Jo and the barrier height, ΦB. Figure 10 shows the current density-voltage (J-V) characteristics for the P3HT/PCBM p-n junction solar cells of both

groups. All device parameters are summarized in 2. From the data a decreasing trend of the PCEs (A 1.78% > B 1.27% > C 0.15%) and fill factor (FF) (A 0.43 > B 0.39 > C 0.32) for Group 1 is observed, the lowest boiling point solvent CH_2Cl_2 is the most promising choice for making solution processed p-n junction OPV devices. The large efficiency drop for the chlorobenzene processed device is related to the extremely thin PCBM layer deposited (~3 nm), in which case a consistent interface is difficult to achieve, which in turn reduces both the open circuit voltage (V_{oc}) and short circuit current (J_{sc}).

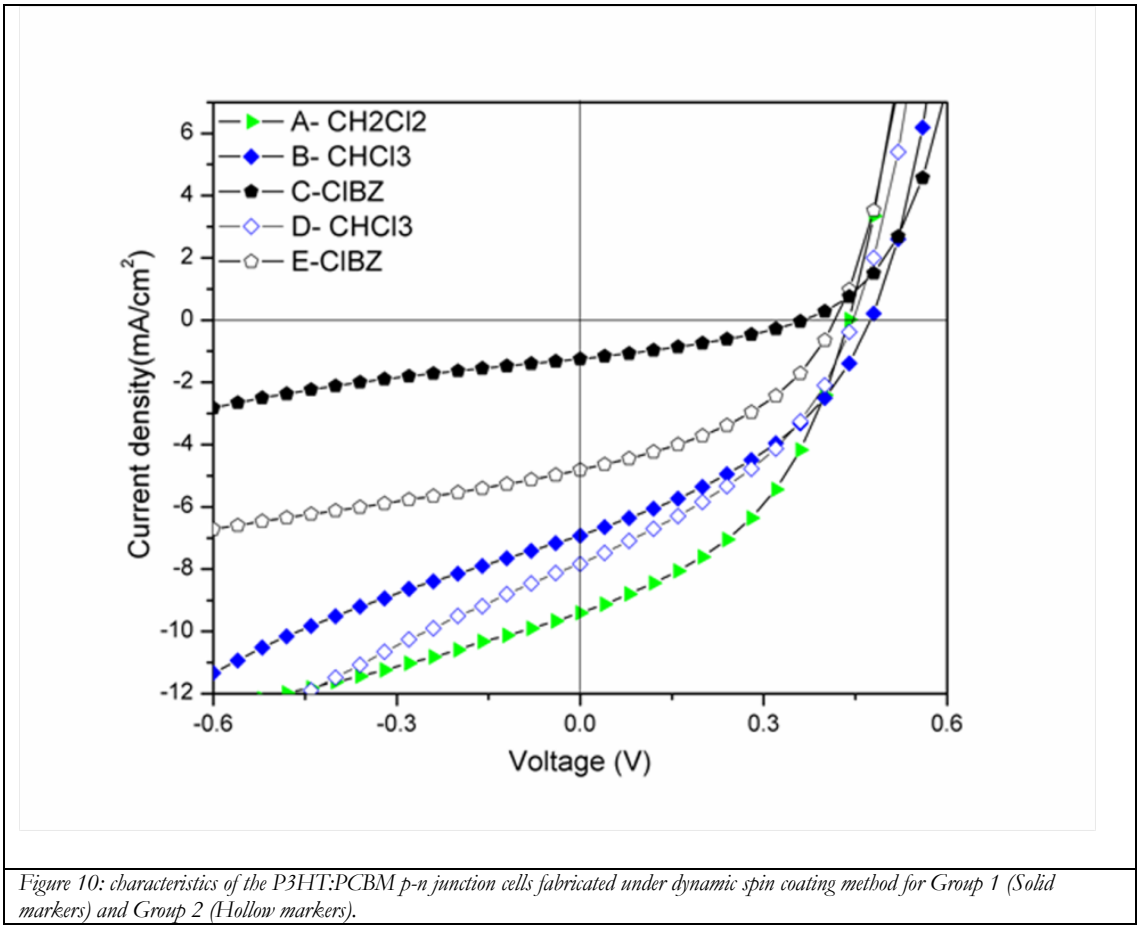

Figure 10: characteristics of the P3HT:PCBM p-n junction cells fabricated under dynamic spin coating method for Group 1 (Solid markers) and Group 2 (Hollow markers).

		Best PCE (%)	Average PCE (n=8)	Voc (V)	Jsc (mA/cm²)	FF
Group 1	A- CH_2Cl_2	1.78	1.50±0.25	0.44	9.40	0.43
	B- $CHCl_3$	1.27	0.84±0.32	0.47	6.89	0.39

	C- chlorobenzene	0.15	0.11±0.03	0.37	1.27	0.32
Group 2	A- CH_2Cl_2	1.78	1.50±0.25	0.44	9.40	0.43
	D- $CHCl_3$	1.34	0.93±0.27	0.45	7.86	0.38
	E- chlorobenzene	0.83	0.49±0.17	0.42	4.80	0.41

Table 0. Summary of device performances of P3HT/PCBM p-n junction photovoltaic devices.

In Group 2, with adjusted P3HT concentration, the P3HT absorbances in $CHCl_3$ and chlorobenzene processed cell are 1.03 and 0.83 (CH_2Cl_2 processed film 0.97), respectively. Besides the decreasing trend in power efficiency (A 1.78% > D 1.34% > E 0.83%), a decreasing trend is also observed in current density, which is directly correlated with exciton dissociation efficiencies resulting from the difference in interface morphology. Given the trend is consistent with the roughness difference in phase images, it is clear that slight change in interface can improve the device performance considerably. The interdigitated morphology obtained through dynamic spin coating successfully resulted in the best device with a PCE 1.78 %, V_{oc} 0.44 V, J_{sc} 9.4 mA/cm^2 and FF of 43%, respectively. Group 2 summarizes all the characteristics of P3HT/PCBM p-n junction photovoltaic devices.

Conclusion

The research presented includes the optical characterization of thin film conjugated polymers and polymer nanocomposites. This characterization was performed via UV-visible absorption and photoluminescence. J-V measurements on the optoelectronic devices were performed in the dark as well as under illumination. Along the way, while studying one of the polymer composites (P3HT:PCBM) measurements (dark and with illumination) and optical absorption spectroscopy. Flat-panel organic photovoltaic devices based upon an active layer composed of a blend of a polymer, poly(3-hexyl-thiophene-2,5-diyl) (P3HT), and functionalized Fullerenes, 1-(3-methoxycarbonyl) propyl-1-phenyl-(6,6) C61 (PCBM) were investigated. These devices were characterized via J-V measurements both in the dark and under white light illumination. The effects of the amount of loading of PCBM (with respect to P3HT), were investigated. Prior to

thermal annealing, two film thickness (120 nm and 170 nm) were tested with different P3HT:PCBM weight loading ratios. From this it was found that the best combination was the 170 nm film with a loading ratio of 1: 0.6 (P3HT:PCBM), resulting in a power conversion efficiency of about 1.78%. It is believed that better stacking methodologies improved dispersion of fullerenes provides more efficient separation and extraction of the excitons.

References

[1] W. Holzer, A. Penzkofer, S.-H. Gong, A. Bleyer and D.D.C. Bradley. Adv. Mater. 8 (**1996**), p. 974.

[2] S. Curran, S. Roth, A.P. Davey, A. Drury, and W. Blau. Synthetic Metals, 83 (**1996**) 239-243

[3] R.H. Friend, R.W. Gymer, A.B. Holmes, J.H. Burroughes, R.N. Marks, C. Taliani, D.D.C. Bradley, D.A. Dos Santos, J.L. Brédas, M. Lögdlund and W.R. Salaneck. Nature 397 (**1999**)

[4] H.W. Kroto, J.R. Heath, S.C. O'Brien, R.F. Curl and R.E. Smalley, Nature 318 (**1985**), pp. 162–163

[5] S. Curran, J. Callaghan, D. Weldon, E. Bourdin, K. Cazzini, W.J. Blau, E. Waldron, D. McGoveran, M. Delamesiere, Y. Sarazin, and C. Hogrel, Electronic Properties of Fullerenes Eds. H. Kuzmany, J. Fink, M. Mehring and S. Roth, Springer Ser. Solid State Sci. 117 (**1993**) 427-433.

[6] S. Curran and S. Roth, In Fullerenes and Fullerene Nanostructures, H. Kuzmany, J. Fink, [2] M. Mehring, and S. Roth, eds. World Scientific, Singapore, New Jersey, London, Hong Kong, (**1996**) 3-13

[7] Y.C. Zhang and X. Wang, International Journal of Solids and Structures, Volume 42, Issue 20, October **2005**, Pages 5399-5412

[8] D-W Pang, Y-D Zhao, P-F Fang, J-K Cheng, Y-Y Chen, Y-P Qi and H D. Abruña, Journal of Electroanalytical Chemistry, 567, 2, **2004**, 339-349

[9] P.M.Ajayan, Nature, Vol 427, 402, 29 Jan **2004**

[10] N.S. Sariciftci, L. Smilowitz, A.J. Heeger and F. Wudl. Science 258 (**1992**), p. 1474

[11] N.S. Sariciftci, Current Opinion in Solid State and Materials Science, 4, 4, **1999**, Pages 373- [12] M. Reyes-Reyes, K. Kim, J. Dewald, R. López-Sandoval, A. Avadhanula, S. Curran and D. L. Carroll, 'Meso-Structure Formation for Enhanced Organic Photovoltaic Cells', Organic Letters, 7, 26, 5749-5752, (**2005**)

[13] S. Doniach, K.K. Chin, I. Lindau et al., Physical Review Letters **58** (6), 591 (**1987**).

[14] A.Y. Cao, V.P. Veedu, X.S. Li et al., Nature Materials **4** (7), 540 (**2005**).

[15] L. Tosheva and V.P. Valtchev, Chemistry of Materials **17** (10), 2494 (**2005**).

[16] S.E. Shaheen, D.S. Ginley, and G.E. Jabbour, Mrs Bulletin **30** (1), 10 (**2005**).

[17] S.R. Forrest, Mrs Bulletin **30** (1), 28 (**2005**).

[18] R.A.J. Janssen, J.C. Hummelen, and N.S. Saricifti, Mrs Bulletin **30** (1), 33 (**2005**).